

Type of the Paper (Article)

## APPLICATION OF RESPONSE SURFACE METHODOLOGY FOR THE OPTIMIZATION OF A COLORIMETRIC DETERMINATION OF AMOXICILLIN

Ounnoughi Chahrazed<sup>a,\*</sup>, Lalaouna Abdeldjalil<sup>b</sup>

<sup>a</sup> Central Laboratory, University Hospital of Sétif, Sétif, Algeria

<sup>b</sup> Laboratory of Analytical Chemistry, Faculty of Medicine, University Salah Boubnider, Constantine 3, Constantine, Algeria

\* Corresponding authors: chahrazed.ounnoughi@univ-setif.dz

### Abstract

A simple and efficient UV-Visible spectrophotometric method was developed and optimized for the quantification of amoxicillin based on the formation of a colored complex with ferric chloride in the presence of hydroxylamine under alkaline conditions. The method relies on the transformation of amoxicillin's  $\beta$ -lactam ring into hydroxamic acid, which forms a stable, colored complex with  $\text{Fe}^{3+}$  ions. A face-centered central composite design (FCCCD) was employed to optimize four critical factors: NaOH concentration,  $\text{Na}_2\text{CO}_3$  concentration, reaction time, and  $\text{FeCl}_3$  concentration. The corrected absorbance was used as the analytical response.

Statistical analysis, including ANOVA, confirmed the significance of the model, with an  $R^2$  of 0.9242 and an adequate precision ratio of 23.056, indicating strong model reliability and signal-to-noise ratio. Numerical optimization was conducted with the objective of maximizing absorbance while minimizing reaction time. The optimal conditions (NaOH 1 N,  $\text{Na}_2\text{CO}_3$  0.6 N, reaction time 10 minutes, and  $\text{FeCl}_3$  15%) yielded a predicted response of 41.799 and a desirability of 0.984. Experimental validation under these conditions showed excellent agreement with the predicted values.

This optimized method offers a reliable, cost-effective, and rapid approach for the quantification of amoxicillin, and may be extended to other  $\beta$ -lactam antibiotics forming hydroxamic acids.

**Keywords:** Amoxicillin, Response Surface Methodology, UV-Visible spectrophotometry, Analytical method optimization

**Citation:** To be added by editorial staff during production.

Academic Editor: First name Last name

Received: date:20/02/2025

Revised: date:15/03/2025

Accepted: date:13/06/2025

Published: date:22/06/2025

**Copyright:** © 2024 by the authors. Submitted publication under the terms and conditions of the Creative Commons

### 1. Introduction:

Amoxicillin (AMX) is a  $\beta$ -lactam antibiotic belonging to the penicillin family, structurally similar to ampicillin and known for its broad-spectrum antimicrobial activity [1]. It is a derivative of 6-aminopenicillanic acid (6-APA), with its distinctiveness from other penicillins stemming from the specific acyl side chain attached to the amino group of the 6-APA core [2]. Amoxicillin trihydrate has the molecular formula  $\text{C}_{16}\text{H}_{19}\text{N}_3\text{O}_5\text{S} \cdot 3\text{H}_2\text{O}$  (Figure 1) and a molecular weight of 419.4 g/mol. It is a white or almost white, crystalline powder, slightly soluble in water, very slightly soluble in ethanol (96 per cent), practically insoluble in fatty oils. It dissolves in dilute acids and dilute solutions of alkali hydroxides [3]. It is widely used to treat various bacterial infections, such as pneumonia and urinary tract infections, due to its ability to inhibit bacterial cell wall synthesis [4]. Although it has good oral bioavailability that is unaffected by food intake, AMT exhibits lower stability in gastric acid due to cleavage of the  $\beta$ -lactam C-N bond, which diminishes its potency and reduces its effective bioavailability [5]. AMX is manufactured in a variety of pharmaceutical forms, such as tablets, capsules, suspensions, and powders [6].

Several analytical methods have been reported in the literature for the quantitative determination of amoxicillin, including spectrofluorimetry [7], capillary electrophoresis[8], voltametric techniques[9], high-performance liquid chromatography (HPLC) [10], ultra-performance liquid chromatography (UPLC)[11], and liquid chromatography tandem mass spectrometry (LC-MS/MS)[12]. The 11th edition of the European Pharmacopoeia specifies a liquid chromatography method for the assay of amoxicillin [3].

However, the use of environmentally hazardous solvents, their high cost, and the time required are among the limitations of the aforementioned methods [13]. Most of these techniques also require instruments that are not available in all research laboratories. Therefore, it was considered necessary to develop a rapid and selective procedure suitable for routine analysis and quality control of the studied drug.

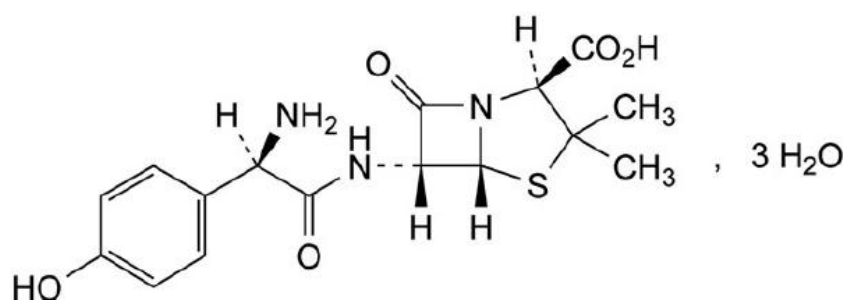


**Figure 1.** Chemical structures of Amoxicillin trihydrate

Ultraviolet-visible (UV-Vis) spectrophotometry offers several advantages over chromatographic techniques: it is faster, consumes fewer solvents, is more cost-effective, and does not require prior sample separation or pretreatment [14].

This study aims to develop novel, environmentally friendly, and cost-effective methods for the estimation of AMX in conventional pharmaceutical formulations, offering rapid, automated, and reliable results with high accuracy, while remaining easy to implement and requiring minimal technical expertise. To optimize and validate these methods efficiently, the Design of Experiments (DoE) methodology is employed, allowing systematic investigation of multiple variables, reduction of experimental runs, and improvement in method robustness and performance.

## 2. Materials and methods

### 2.1. Apparatus and software

The measurements were performed using a Thermo Scientific UV-Visible spectrophotometer, model GENESYS 10S (Madison, Wisconsin, USA), equipped with a 1 cm quartz cell and connected to an HP-compatible computer running VISIONlite software version 5.1.

The Design Expert 13 software (Trial version, Stat-Ease Inc) was used to analyze the response surface.

### 2.2. Reagents and chemicals

Standards of AMX used with analytical-grade from Merck (Darmstadt, Germany) with purities of 100.8%.

Sodium hydroxide (NaOH) was obtained from Sigma-Aldrich, and sodium carbonate (Na<sub>2</sub>CO<sub>3</sub>) was purchased from Cheminova. Ferric chloride (FeCl<sub>3</sub>) was

supplied by Riedel-de Haën, while hydroxylamine hydrochloride ( $\text{NH}_2\text{OH}\cdot\text{HCl}$ ) was sourced from Fluka Analytical. Hydrochloric acid ( $\text{HCl}$ ) was provided by Biochem. All reagents were of analytical grade and used without further purification.

### 2.3. Method development

The principle of the assay reaction is based on the fact that acyl compounds react with hydroxylamine to form hydroxamic acids. These acids act as bidentate chelators that form strong complexes with Fe (III), resulting in a colored complex that can be quantified using UV-Visible spectroscopy.

In the presence of hydroxylamine, the acyl group in the amoxicillin structure is released through the opening of the  $\beta$ -lactam ring, leading to the formation of a hydroxamic acid. This ability to form a colored complex with iron has been utilized for the spectrophotometric determination of amoxicillin trihydrate in the visible range [15].

A solution of amoxicillin was prepared by reacting 30 mg of amoxicillin with a reagent mixture containing 1 ml of 0.4 N hydroxylamine hydrochloride ( $\text{NH}_2\text{OH}$ ), sodium hydroxide ( $\text{NaOH}$ ), sodium carbonate ( $\text{Na}_2\text{CO}_3$ ), and, subsequently, hydrochloric acid ( $\text{HCl}$ ) and ferric chloride ( $\text{FeCl}_3$ ) as chromogenic agents. Specifically, 0.6 ml of  $\text{NaOH}$  (0.8 N), 0.4 ml of  $\text{Na}_2\text{CO}_3$ , and 1 ml of  $\text{NH}_4\text{OH}$  (0.4 N) were added to the amoxicillin. After a reaction time of 20 minutes, 2.5 ml of 2 N  $\text{HCl}$  and 2.5 ml of 10%  $\text{FeCl}_3$  were added successively. The final volume was made up to 50 ml with distilled water. The absorbance of the resulting colored solution was measured using a UV-Visible spectrophotometer.

### 2.4. Experimental design and optimization

To optimize the reaction conditions for the colorimetric determination of amoxicillin, a face-centered central composite design (FCCCD) was employed. This design enables the evaluation of linear, interaction, and quadratic effects of multiple factors on a response variable, with a reduced number of experimental runs. It is particularly well suited for sequential experimentation and allows the integration of information from prior factorial designs through the addition of axial and center points.

In this study, four independent variables were selected based on preliminary experiments and chemical knowledge of the system, as they were expected to significantly influence the formation and intensity of the colored complex resulting from the reaction between amoxicillin, hydroxylamine, and ferric chloride. These variables were:  $\text{NaOH}$  concentration, varied between 0.6 and 1.0 N;  $\text{Na}_2\text{CO}_3$  concentration, between 0.2 and 0.6 N; reaction time, from 10 to 30 minutes; and  $\text{FeCl}_3$  concentration, from 5% to 15%. The different levels of the selected factors are presented in Table 1.

**Table 1.** Variables and their experimental design levels

Independent variables	Coded symbols	Levels		
		-1	0	1
$\text{NaOH}$ concentration (N)	A	0.6	0.8	1
$\text{Na}_2\text{CO}_3$ concentration (N)	B	0.2	0.4	0.6
Reaction time (min)	C	10	20	30
$\text{FeCl}_3$ concentration (%)	D	5	10	15

The response variable was the absorbance corrected ( $A_c$ ) based on the exact mass of amoxicillin used in each trial. This correction ensures that variations in sample weight do not bias the assessment of the factors' effects and allows for a more accurate comparison across all experimental runs.

A total of 30 experiments were carried out, including 16 factorial points, 8 axial points (with  $\alpha = \pm 1$ ), and 6 replicates at the center point to assess the experimental error and model adequacy. The experimental design was generated and analyzed using Design Expert 13 software (Trial version, Stat-Ease Inc). The experiments were randomized to minimize the effects of uncontrolled variables and results are presented in Table 2.

**Table 2.** Central composite matrix design with four independent variables and measured response.

Experimental run	A	B	C	D	Response
1	-1	-1	-1	-1	20.1701
2	1	-1	-1	-1	26.7208
3	-1	1	-1	-1	8.21549
4	1	1	-1	-1	12.1854
5	-1	-1	1	-1	20.3974
6	1	-1	1	-1	29.3688
7	-1	1	1	-1	22.7425
8	1	1	1	-1	30.903
9	-1	-1	-1	1	34.5098
10	1	-1	-1	1	39.2359
11	-1	1	-1	1	37.1096
12	1	1	-1	1	42.8808
13	-1	-1	1	1	31.7822
14	1	-1	1	1	36.0066
15	-1	1	1	1	33.0693
16	1	1	1	1	41.4803
17	-1	0	0	0	27.4667
18	1	0	0	0	36.3366
19	0	-1	0	0	29.3645
20	0	1	0	0	35.5082
21	0	0	-1	0	31.5947
22	0	0	1	0	30.3909
23	0	0	0	-1	23.5831
24	0	0	0	1	34.3894
25	0	0	0	0	31.2787
26	0	0	0	0	34.8355
27	0	0	0	0	34.7333
28	0	0	0	0	33.3444
29	0	0	0	0	34.4262
30	0	0	0	0	34.8208

## 2.5. Statistical analysis

The experimental data obtained from the FCCCD were subjected to statistical analysis using Design-Expert® software. A second-order polynomial model was applied to describe the effects of the experimental factors and their interactions on the response. The model included linear, quadratic, and interaction terms, and was expressed in coded variables according to the following general form:

$$y = \beta_0 + \sum_{i=1}^k \beta_i x_i + \sum_{i=1}^k \beta_{ii} x_i^2 + \sum_{i=1}^{k-1} \sum_{j=i+1}^k \beta_{ij} x_i x_j + \varepsilon$$

where  $y$  is the predicted response,  $\beta_0$  is the intercept,  $\beta_i$  are the linear coefficients,  $\beta_{ii}$  are the quadratic coefficients,  $\beta_{ij}$  are the interaction coefficients, and  $\varepsilon$  is the residual error. The variables  $x_i$  and  $x_j$  represent the coded levels of the independent factors [16].

The significance and adequacy of the model were evaluated using analysis of variance (ANOVA). Several statistical parameters were considered, including the F-value to assess overall model significance, and p-values to determine the significance of individual terms (linear, quadratic, and interaction effects). The coefficient of determination ( $R^2$ ), adjusted  $R^2$ , and predicted  $R^2$  were used to evaluate the model's descriptive and predictive capabilities. The lack-of-fit test was applied to verify whether the model appropriately fit the experimental data, and the adequate precision value was calculated to assess the signal-to-noise ratio, with values above 4 indicating adequate model discrimination. Only terms with a p-value less than 0.05 were considered statistically significant, and non-significant terms were excluded when necessary to improve the model's performance.

### 3. Results and discussion

#### 3.1. Effect of Individual Factors on the Response Variable

The influence of each individual factor on the corrected absorbance ( $A_c$ ) was assessed by plotting the response against the levels of the corresponding variable, while keeping the other factors constant at their central values (Figure 2).

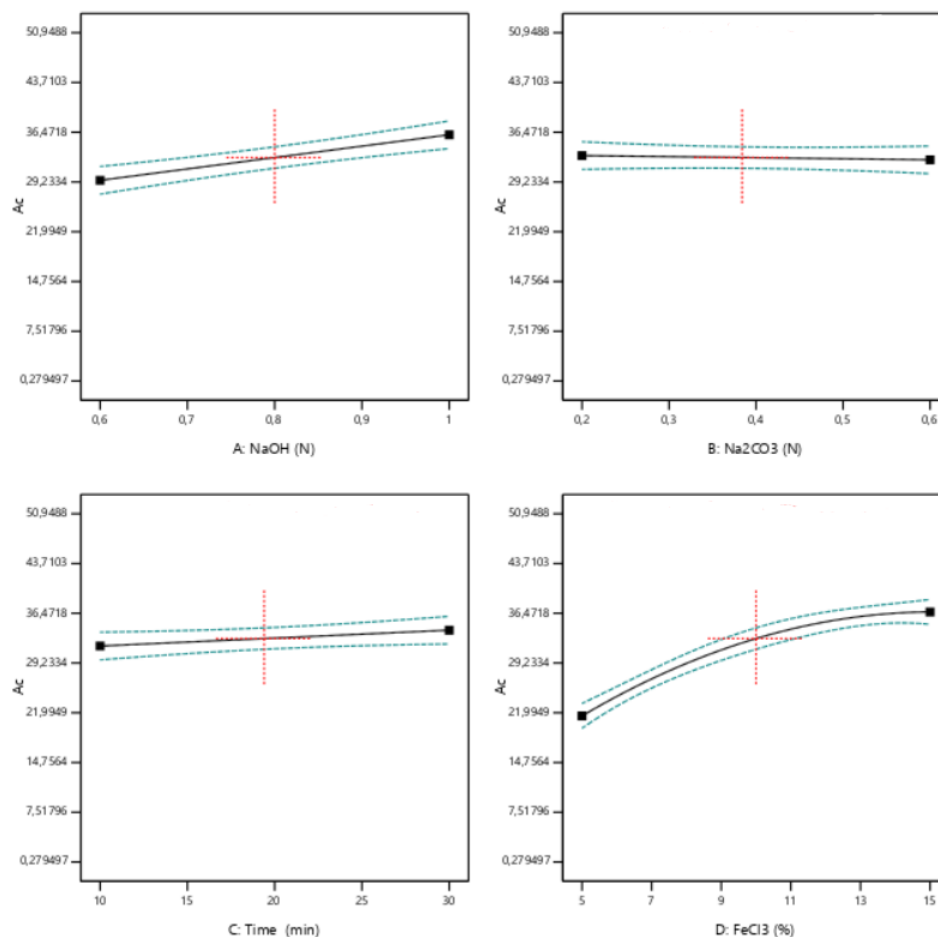


**Figure 2.** Effect of individual factors on the corrected absorbance (Ac): (A) NaOH concentration, (B) Na<sub>2</sub>CO<sub>3</sub> concentration, (C) Reaction time, and (D) FeCl<sub>3</sub> concentration.

The observed increase in absorbance with rising NaOH concentration suggests a favorable effect of the alkaline medium on the progression of the reaction. NaOH likely facilitates the opening of the  $\beta$ -lactam ring of amoxicillin under the action of hydroxylamine (NH<sub>4</sub>OH), leading to the formation of hydroxamic acid derivatives. These intermediates are known to form stable colored complexes with Fe<sup>3+</sup> ions, explaining the enhanced signal at higher NaOH concentrations.

The Na<sub>2</sub>CO<sub>3</sub> concentration had minimal influence on the absorbance across the tested range. As a milder base compared to NaOH, Na<sub>2</sub>CO<sub>3</sub> may primarily act as a buffer in the reaction medium, but does not significantly affect the hydrolysis of the  $\beta$ -lactam ring or the subsequent complexation process.

The reaction time showed a slight positive effect on absorbance, with higher values observed at longer durations. This trend indicates that the formation of hydroxamic acid and its complexation with ferric ions is time-dependent, although the process appears to approach equilibrium within the studied time range.

A pronounced increase in absorbance was recorded with increasing FeCl<sub>3</sub> concentration, especially between 5% and 10%, beyond which the response tended to plateau. This confirms the critical role of Fe<sup>3+</sup> in the complexation process, as ferric ions react with the hydroxamic acid moiety to form a stable colored complex. The saturation beyond 10% suggests that excess Fe<sup>3+</sup> does not enhance the response further, likely due to complete complexation of available ligands.

These results align with the established chemical behavior of penicillins, wherein the  $\beta$ -lactam ring is prone to nucleophilic attack. Under alkaline conditions,

hydroxylamine (NH<sub>4</sub>OH) facilitates the cleavage of the β-lactam ring, leading to the formation of hydroxamic acid derivatives. These hydroxamic acids are known to form stable, colored complexes with ferric ions (Fe<sup>3+</sup>), a reaction that can be effectively monitored using UV-Visible spectrophotometry due to the characteristic absorption bands of the resulting complexes [17] [18].

### 3.2. Optimization of the procedure

#### 3.2.1. Model fitting and statistical analysis

The experimental results were analyzed using a reduced quadratic model to investigate the influence of four critical factors: NaOH concentration (A), Na<sub>2</sub>CO<sub>3</sub> concentration (B), reaction time (C), and FeCl<sub>3</sub> concentration (D) on the corrected absorbance (Ac) of the amoxicillin-hydroxylamine-FeCl<sub>3</sub> complex. The model fitting was evaluated through analysis of variance (ANOVA), and the statistical parameters are summarized in Table 3.

Based on the ANOVA results, insignificant terms were removed to improve the model. The final reduced quadratic equation for corrected absorbance (Ac), expressed in coded variables, is:

$$A_c = 32.84 + 3.31A - 0.1923B + 1.31C + 7.57D + 1.93 BC + 2.23 BD - 2.97CD - 3.69D^2$$

Positive coefficients (A, C, D, BC, BD) indicate that increasing these factors or interactions tends to increase the response, whereas negative coefficients (B, CD, D<sup>2</sup>) suggest an inverse effect on absorbance. The model F-value of 30.55 and the very low p-value (< 0.0001) confirm the model's high significance. Significant terms (p < 0.05) include A, C, D, BC, BD, CD, and D<sup>2</sup>.

No significant lack of fit was observed (p = 0.0619), confirming that the model fits the experimental data appropriately. The coefficient of determination (R<sup>2</sup> = 0.9209) indicates that 92.09% of the variability in the response is explained by the model.

The adjusted R<sup>2</sup> (0.8907) and predicted R<sup>2</sup> (0.8051) are in good agreement, with a difference below 0.2, supporting the model's predictive capacity. Moreover, the Adequate Precision value of 23.06 confirms a strong signal-to-noise ratio, far above the minimum desirable threshold of 4.

These statistical indicators confirm the reliability and robustness of the model for exploring and optimizing the experimental space. The correlation between actual and predicted absorbance values is also illustrated in Figure 3, where the close alignment of data points along the diagonal indicates strong predictive accuracy.



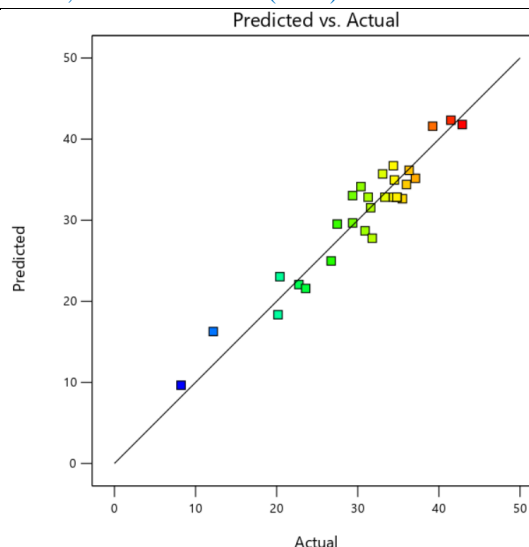


**Figure 3.** Plot of predicted vs. actual values for the corrected absorbance ( $A_c$ )

### 3.2.2. Response Surface Interpretation

The effects of the investigated variables on the response ( $A_c$ ) were further analyzed using three-dimensional response surface plots and their corresponding contour plots, as shown in Figure 4 (a–f). Such graphical representations illustrate the influence of two factors on the response while other two factors are held constant at their center levels, allowing for the visualization of both main and interaction effects within the experimental domain.

In **Figure 4a**, the interaction between NaOH and  $\text{Na}_2\text{CO}_3$  concentrations reveals that variations in  $\text{Na}_2\text{CO}_3$  do not substantially affect the response, while an increase in NaOH leads to a notable enhancement in  $A_c$ . The corresponding contour lines are nearly vertical, indicating a dominant effect of NaOH and minimal influence from  $\text{Na}_2\text{CO}_3$ . **Figure 4b** depicts the combined effect of NaOH concentration and reaction time. Both variables contribute positively to  $A_c$ , with NaOH again playing the more prominent role. The slightly inclined contour lines suggest a mild interaction between these factors, with a gradual increase in response at higher values.

The 3D and contour plots in **Figure 4c** illustrate a strong synergistic effect between NaOH (A) and  $\text{FeCl}_3$  (D) on the response  $A_c$ . As both factors increase, a pronounced rise in  $A_c$  is observed. The response surface shows a curved upward trend, especially at high levels of  $\text{FeCl}_3$  and NaOH, indicating their combined positive influence. The contour plot reveals elliptical contours, further emphasizing this strong interaction, with  $\text{FeCl}_3$  exhibiting a particularly dominant effect on enhancing  $A_c$ .

The 3D and contour plots in **Figure 4d** show the combined influence of  $\text{Na}_2\text{CO}_3$  concentration (B) and reaction time (C) on the response  $A_c$ . While  $\text{Na}_2\text{CO}_3$  alone appears to have a minimal effect, the interaction with time reveals a modest increase in  $A_c$ , particularly at longer durations and higher  $\text{Na}_2\text{CO}_3$  concentrations. The curvature of the response surface and the slight gradient in the contour plot suggest a subtle synergistic effect between the two factors, though less pronounced compared to other interactions.



**Table3.** ANOVA analysis for the quadratic model of the corrected absorbance of the amoxicillin-hydroxylamine-FeCl<sub>3</sub> complex

Source	Sum of Squares	df	Mean Square	F-value	p-value
<b>Model</b>	1637.34	8	204.67	30.55	< 0.0001
A-NaOH	197.71	1	197.71	29,51	< 0.0001
B-Na <sub>2</sub> CO <sub>3</sub>	0.6656	1	0.6656	0.0994	0.7557
C-Time	30.73	1	30.73	4.59	0.0441
D-FeCl <sub>3</sub>	1030.24	1	1030.24	153.79	< 0.0001
BC	59.62	1	59.62	8.90	0.0071
BD	79.28	1	79.28	11.83	0.0025
CD	141.12	1	141.12	21.07	0.0002
D <sup>2</sup>	97.98	1	97.98	14.63	0.0010
<b>Residual</b>	140.68	21	6.70		
Lack of Fit	130.81	16	8.18	4.14	0.0619
Pure Error	9.87	5	1.97		
Total	1778.02	29			
*R <sup>2</sup>	0.9209				
*R <sup>2</sup> . adj	0.8907				
*R <sup>2</sup> pred	0.8051				
Adeq. Precision	23.05				
C.V. %	8.45				

df: Degree of freedom. X1: solvent-to-solid ratio (mL/g);

\*R<sup>2</sup>, \*R<sup>2</sup> pred and \*R<sup>2</sup>. adj are calculated for the reduced model.

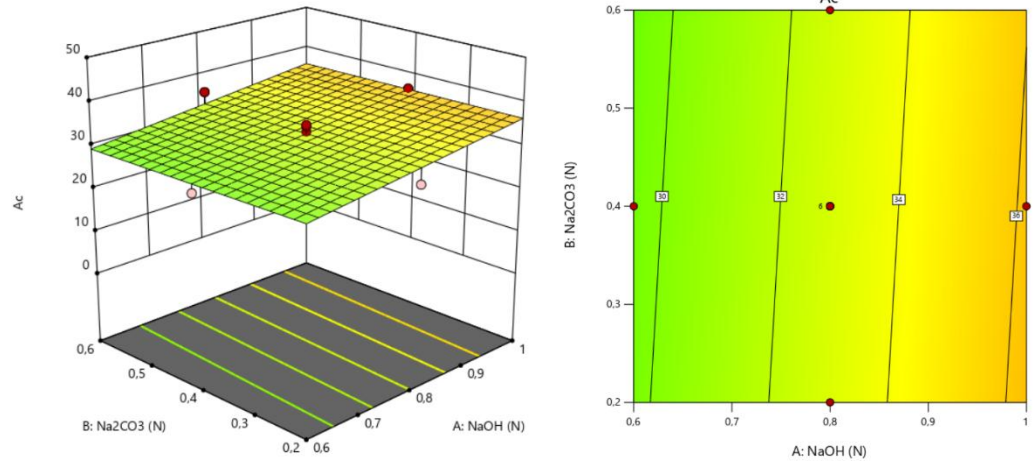
C.V. % coefficient of variation.

**Figure 4e** illustrates the 3D surface response and contour plots representing the combined effect of FeCl<sub>3</sub> concentration (D) and Na<sub>2</sub>CO<sub>3</sub> concentration (B) on the response A<sub>c</sub>, while the remaining factors are held constant at their central levels. From the 3D surface plot, it is evident that the response A<sub>c</sub> increases significantly with increasing FeCl<sub>3</sub> concentration. The surface exhibits a steep gradient along the FeCl<sub>3</sub> axis, indicating a strong positive influence of this factor. In contrast, the effect of Na<sub>2</sub>CO<sub>3</sub> remains relatively minor, as the surface remains nearly flat in the B direction. The contour plot confirms this observation, showing nearly horizontal contour lines. This orientation suggests that variations in FeCl<sub>3</sub> drive the changes in the response, whereas Na<sub>2</sub>CO<sub>3</sub> has a limited impact in the explored range. The highest values of A<sub>c</sub> are observed at the upper levels of FeCl<sub>3</sub>, regardless of the Na<sub>2</sub>CO<sub>3</sub> concentration. This aligns with the statistical analysis that identified FeCl<sub>3</sub> as the most influential factor in the model.

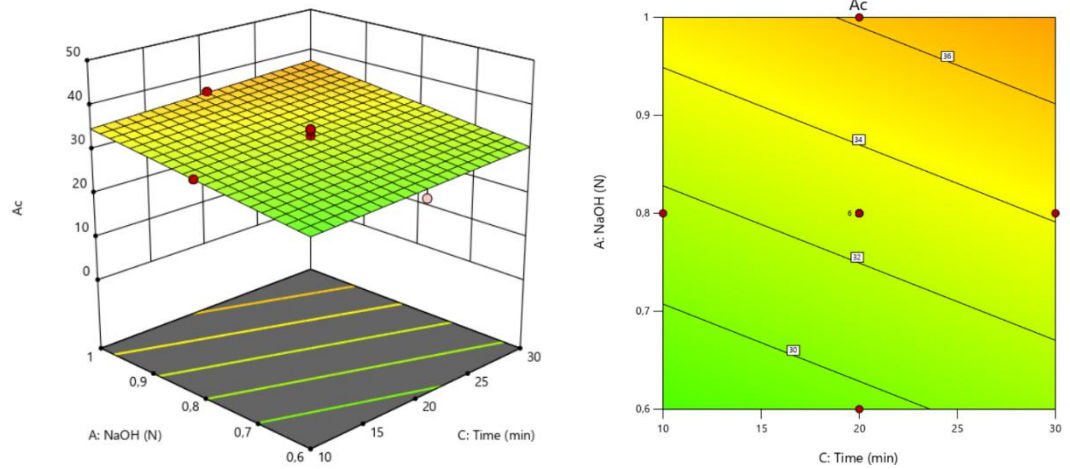
In **Figure 4f** the 3D surface plot shows that an increase in FeCl<sub>3</sub> concentration leads to a significant enhancement in A<sub>c</sub>, whereas reaction time exhibits a comparatively moderate effect. The surface tilts more steeply along the FeCl<sub>3</sub> axis, confirming its dominant influence on the response. In the contour plot, the nearly

horizontal contour lines indicate that variations in  $Ac$  are primarily driven by changes in  $FeCl_3$  concentration. Reaction time contributes slightly to the response, with a gentle upward trend observed. The maximum  $Ac$  values are observed at higher  $FeCl_3$  levels, regardless of time, highlighting  $FeCl_3$  as a critical factor in the reaction process.

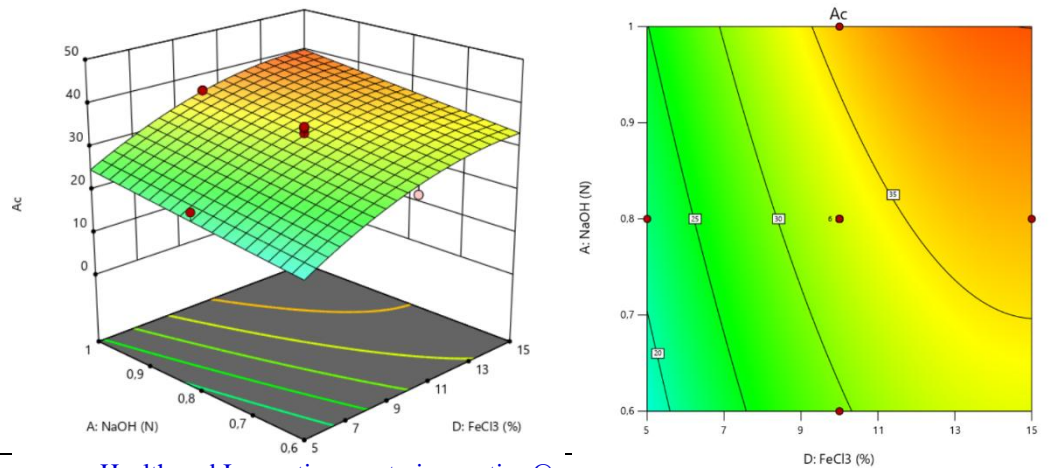
a



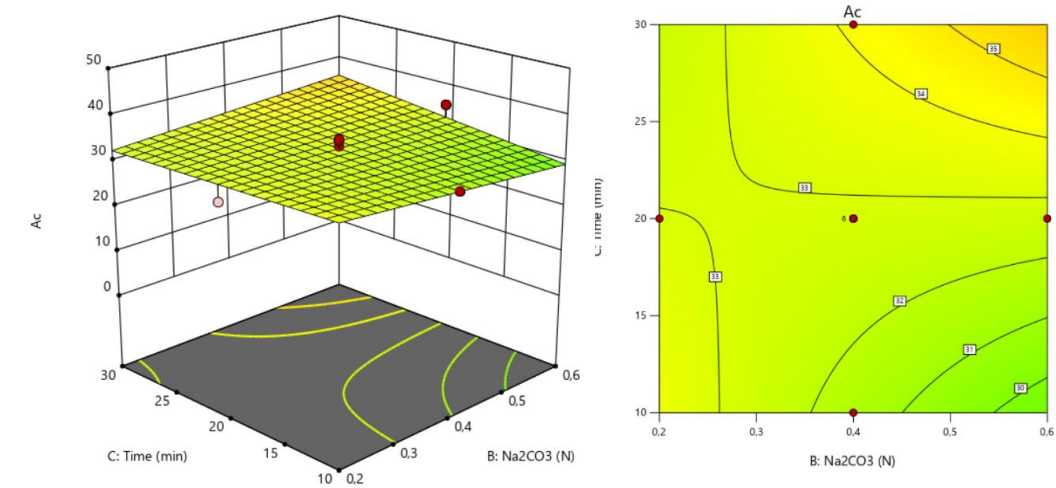
b



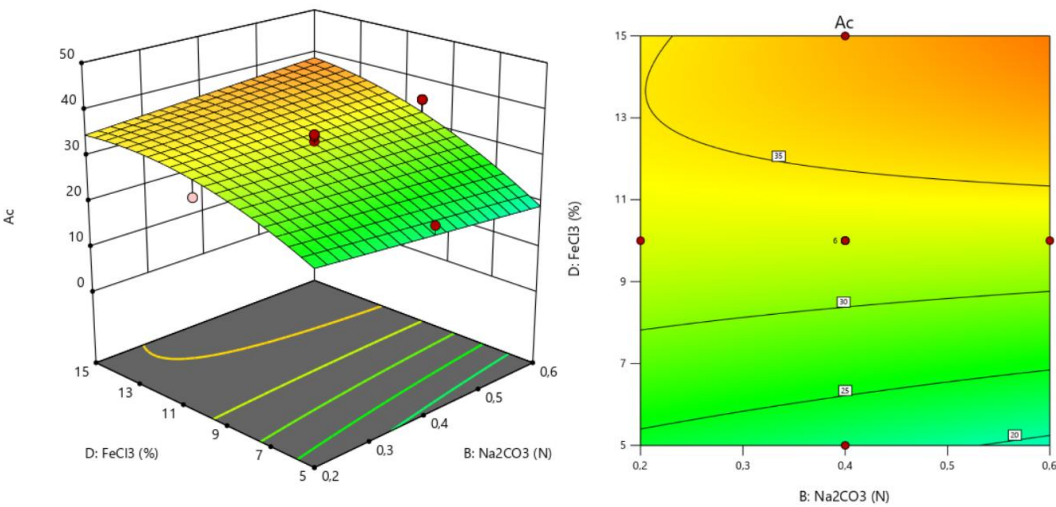
c



d



e



f

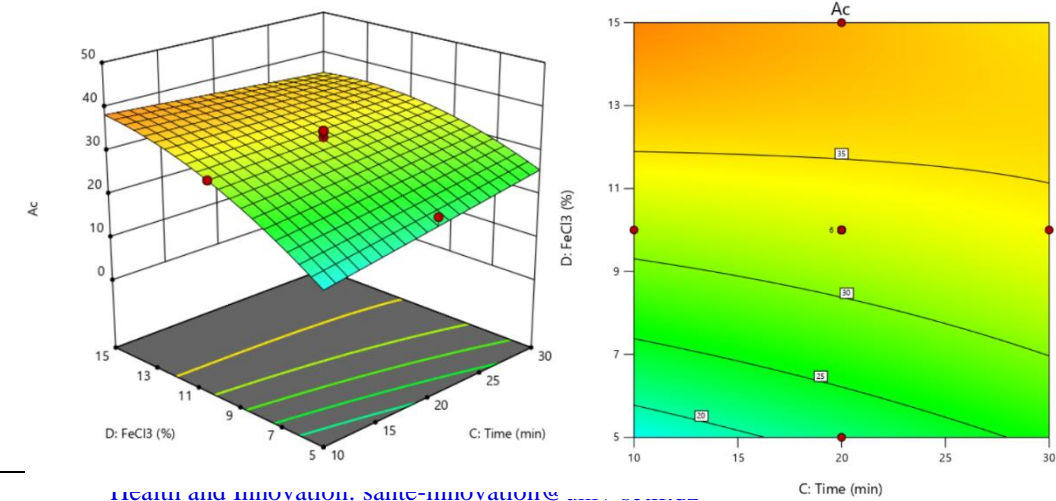


**Figure 4 (a-f).** 3D response surface plots and corresponding contour plots illustrating the combined effects of the studied variables on the corrected absorbance ( $A_c$ ) of the amoxicillin-hydroxylamine-ferric chloride complex: (a) NaOH and  $\text{Na}_2\text{CO}_3$  concentrations, (b) NaOH concentration and reaction time, (c) NaOH and  $\text{FeCl}_3$  concentrations, (d)  $\text{Na}_2\text{CO}_3$  concentration and reaction time, (e)  $\text{Na}_2\text{CO}_3$  and  $\text{FeCl}_3$  concentrations, and (f) reaction time and  $\text{FeCl}_3$  concentration.

### 3.3. Numerical Optimization and Model Validation

Numerical optimization was carried out using the desirability function approach to identify the best combination of experimental factors that would maximize the corrected absorbance ( $A_c$ ) of the amoxicillin-hydroxylamine- $\text{FeCl}_3$  complex while minimizing the reaction time. Based on this dual-objective optimization, the optimal conditions were determined as follows: NaOH concentration of 1 N,  $\text{Na}_2\text{CO}_3$  concentration of 0.6 N, reaction time of 10 minutes, and  $\text{FeCl}_3$  concentration of 15%. Under these conditions, the model predicted a corrected absorbance of 41.80, with an overall desirability of 0.984, indicating a highly satisfactory compromise between the two objectives.

To validate the predictive accuracy of the model, the experiment was conducted in triplicate under the optimized conditions. The mean observed absorbance was 42.99, which falls within the 95% prediction interval (36.99 to 46.61) provided by the model. This close agreement between predicted and experimental values confirms the validity and robustness of the optimization model. The detailed results of the model validation, including the predicted and observed responses, standard deviation, and prediction intervals, are summarized in Table 4.

**Table 4.** Predicted and experimental values of responses at the optimum values of NaOH concentration (1 N),  $\text{Na}_2\text{CO}_3$  concentration (0.6 N), reaction time (10 min), and  $\text{FeCl}_3$  concentration (15%).

Response	Predicted value	95 % CI low*	95 % CI high**	Experimental mean value
Corrected absorbance ( $A_c$ )	41.80	36.99	46.61	42.99±0.99

\* 95 % CI low is the lower limit of the 95 % confidence interval.

\*\* 95 % CI high is the upper limit of the 95 % confidence interval.

The results demonstrate that the chosen experimental conditions offer a reliable and efficient method for maximizing color intensity within a reduced reaction time, making the procedure suitable for practical analytical applications.

### Conclusion

In this study, a simple, sensitive, and optimized UV-Visible spectrophotometric method was developed for the quantification of amoxicillin based on its complexation reaction with ferric chloride in the presence of hydroxylamine. A face-centered central composite design (FCCCD) was successfully employed to investigate and optimize the influence of four key experimental factors: NaOH concentration,  $\text{Na}_2\text{CO}_3$  concentration, reaction time, and  $\text{FeCl}_3$  concentration. The corrected absorbance was used as the response to evaluate the formation of the colored complex.

Statistical analysis confirmed the significance and reliability of the quadratic model, with a high coefficient of determination ( $R^2 = 0.9242$ ) and a non-significant lack of fit, indicating good agreement between the predicted and experimental values. The optimized conditions (NaOH 1 N,  $\text{Na}_2\text{CO}_3$  0.6 N, reaction time 10 min, and  $\text{FeCl}_3$  15%) led to a high corrected absorbance, with a desirability value of 0.984, confirming the model's robustness and predictive capability. Validation experiments demonstrated excellent reproducibility and consistency with model predictions.

This optimized method can be considered a valuable analytical tool for the quantification of amoxicillin or related  $\beta$ -lactam antibiotics based on hydroxamic acid complexation, offering rapid analysis, low reagent consumption, and good sensitivity.

### Declaration of links of interest

The authors declare having no conflicts in interests.

### References

1. Asres E, Layloff T, Ashenef A. Development and validation of a high-performance thin layer chromatography method for the simultaneous determination of amoxicillin and clavulanic acid combinations in tablet dosage forms. *Heliyon* [Internet]. déc 2023 [cité 3 mai 2025];9(12):e22891. Disponible sur: <https://linkinghub.elsevier.com/retrieve/pii/S2405844023100995>
2. De Rosa M, Vigliotta G, Palma G, Saturnino C, Soriente A. Novel Penicillin-Type Analogues Bearing a Variable Substituted 2-Azetidinone Ring at Position 6: Synthesis and Biological Evaluation. *Molecules* [Internet]. 10 déc 2015 [cité 10 mai 2025];20(12):22044– 57. Disponible sur: <https://www.mdpi.com/1420-3049/20/12/19828>
3. European Directorate for the Quality of Medicines & HealthCare. *European Pharmacopoeia*. 11<sup>e</sup> éd. Strasbourg; 2023.
4. Oday J, Hadi H, Hashim P, Richardson S, Iles A, Pamme N. Development and validation of spectrophotometric method and paper-based microfluidic devices for the quantitative determination of Amoxicillin in pure form and pharmaceutical formulations. *Heliyon* [Internet]. févr 2024 [cité 3 mai 2025];10(3):e24968. Disponible sur: <https://linkinghub.elsevier.com/retrieve/pii/S240584402400999X>
5. Hoang Vu D, Giang Do T. Comparative Study of RP-HPLC and UV Spectrophotometric Techniques for the Simultaneous Determination of Amoxicillin and Cloxacillin in Capsules. *J Young Pharm* [Internet]. avr 2010 [cité 10 mai 2025];2(2):190– 5. Disponible sur: <http://linkinghub.elsevier.com/retrieve/pii/S0975148310220149>
6. Falih MS, Abbas RF, Mahdi NI, Abood NK, Hassan MJM. FIA- spectrophotometric method for the determination of amoxicillin in pharmaceuticals; application of AES, GAPI, and AGREE greenness assessment tools. *MethodsX* [Internet]. déc 2023 [cité 10 mai 2025];11:102437. Disponible sur: <https://linkinghub.elsevier.com/retrieve/pii/S2215016123004338>
7. Davidson DF. A simple chemical method for the assay of amoxycillin in serum and urine. *Clin Chim Acta* [Internet]. mai 1976 [cité 10 mai 2025];69(1):67– 71. Disponible sur: <https://linkinghub.elsevier.com/retrieve/pii/0009898176904721>
8. Hancu G, Neacșu A, Papp LA, Ciurba A. Simultaneous determination of amoxicillin and clavulanic acid in pharmaceutical preparations by capillary zone electrophoresis. *Braz J Pharm Sci* [Internet]. juin 2016 [cité 10 mai 2025];52(2):281– 6. Disponible sur: [http://www.scielo.br/scielo.php?script=sci\\_arttext&pid=S1984-82502016000200281&lng=en&tlng=en](http://www.scielo.br/scielo.php?script=sci_arttext&pid=S1984-82502016000200281&lng=en&tlng=en)
9. Valenga MGP, Felsner ML, De Matos CF, De Castro EG, Galli A. Development and validation of voltammetric method for determination of amoxicillin in river water. *Anal Chim Acta* [Internet]. nov 2020 [cité 10 mai 2025];1138:79– 88. Disponible sur: <https://linkinghub.elsevier.com/retrieve/pii/S0003267020309417>
10. Bellur Atici E, Yazar Y, Ağtaş Ç, Ridvanoğlu N, Karlığa B. Development and validation of stability indicating HPLC methods for related substances and assay analyses of amoxicillin and potassium clavulanate mixtures. *J Pharm Biomed Anal* [Internet]. mars 2017 [cité 10 mai 2025];136:1– 9. Disponible sur: <https://linkinghub.elsevier.com/retrieve/pii/S0731708516315047>



11. Uddin MN, Das S, Khan SH, Shill SK, Bhuiyan HR, Karim R. Simultaneous determination of amoxicillin and chloramphenicol and their drug interaction study by the validated UPLC method. *J Taibah Univ Sci* [Internet]. sept 2016 [cité 10 mai 2025];10(5):755- 65. Disponible sur: <https://www.tandfonline.com/doi/full/10.1016/j.jtusci.2015.11.005>
12. Gaikwad A, Gavali S, Narendiran, Katale D, Bonde S, Bhadane RP. An LC–MS–MS method for the simultaneous quantification of amoxicillin and clavulanic acid in human plasma and its pharmacokinetic application. *J Pharm Res* [Internet]. août 2013 [cité 10 mai 2025];6(8):804- 12. Disponible sur: <https://linkinghub.elsevier.com/retrieve/pii/S0974694313003010>
13. Valizadeh M, Sohrabi MR, Motiee F. The application of continuous wavelet transform based on spectrophotometric method and high-performance liquid chromatography for simultaneous determination of anti-glaucoma drugs in eye drop. *Spectrochim Acta A Mol Biomol Spectrosc* [Internet]. déc 2020 [cité 10 mai 2025];242:118777. Disponible sur: <https://linkinghub.elsevier.com/retrieve/pii/S1386142520307563>
14. Salehian S, Sohrabi MR, Davallo M. Rapid and simple spectrophotometric method using feedforward backpropagation and radial basis function neural networks for the simultaneous determination of amoxicillin and clavulanic acid in commercial tablet and human blood serum. *Optik* [Internet]. déc 2021 [cité 10 mai 2025];247:167908. Disponible sur: <https://linkinghub.elsevier.com/retrieve/pii/S0030402621014856>
15. Davidson DF. A simple chemical method for the assay of amoxycillin in serum and urine. *Clin Chim Acta* [Internet]. mai 1976 [cité 5 juin 2022];69(1):67- 71. Disponible sur: <https://linkinghub.elsevier.com/retrieve/pii/0009898176904721>
16. Myers RH. *Response Surface Methodology: Process and Product Optimization Using Designed Experiments*. 1st ed. Newark: John Wiley & Sons, Incorporated; 2016. 1 p. (New York Academy of Sciences Series).
17. Sow IS. Methods for synthesizing hydroxamic acids and their metal complexes. *Eur J Chem* [Internet]. 31 déc 2024 [cité 17 mai 2025];15(4):345- 54. Disponible sur: <https://www.eurjchem.com/index.php/eurjchem/article/view/2565>
18. Nenortiene P, Sapragoniene M, Stankevicius A. [Synthesis of hydroxamic acids and study of their complexes with iron (II) and (III) ions]. *Med Kaunas Lith*. 2002;38(7):744- 51.